ISSN(Online) : 2319 - 8753
ISSN (Print) : 2347 - 6710

International Journal of Innovative Research in Science, Engineering and Technology

(An ISO 3297: 2007 Certified Organization)

Vol. 4, Issue 2, February 2015

Synthesis, Characterization, Electrochemical Behaviour, DNA Binding and Cleavage Studies of Substituted β-DiketimineCopper(II) and Zinc(II) Complexes

Ramaraj Jeyamurugan[1], Natarajan Raman[2]

Assistant Professor, Department of Chemistry, Dr.Zakir Husain College, Ilayangudi, Tamil Nadu, India[1]

Associate Professor, Department of Chemistry, VHNSN College, Virudhunagar, Tamil Nadu, India[2]

ABSTRACT: Several novel copper(II) and zinc(II) complexes have been synthesized from Schiff base(s) obtained by the condensation of Knoevenagel condensate, 3-(3-phenyl-allylidene)-pentane-2,4-dione with *p*-substituted (X) aniline where X = $–NO_2$ (L^1), –H (L^2), –OH (L^3) and $–OCH_3$ (L^4)] and, copper(II) chloride/zinc(II) chloride. They have been characterized by analytical and spectral techniques. Electronic absorption and electrochemicalmeasurements prove that the complexes intercalate into DNA. Control DNA cleavage experiments using pUC19 supercoiled (SC) DNA and minor groove binder (distamycin) suggest the minor groove binding tendency for the synthesized complexes.

KEYWORDS: Knoevenagel condensate, complexes, DNA binding, DNA cleavage, cyclic voltammetry.

I. INTRODUCTION

Transition metals are essential for the normal functioning of living organisms. Therefore, it is not surprising that transition metal compounds are of great interest as potential drugs [1]. The low molecular weight transition metal complexes with their versatile structures, redox behaviour and physicochemical properties are found to be useful as highly sensitive diagnostic agents and the metal or ligands in the complexes can be varied in an easily controlled way to facilitate individual application [2].

Deoxyribonucleic acid (DNA) is the primary target molecule for the most anticancer and antiviral therapies according to cell biology [3]. DNA-metal complex interaction has become subject of intense research. This interaction is essentially non-covalent, either by intercalation, groove binding or external electrostatic binding. The binding of DNA to metal complex is closely related to the structure of the complex [4]. Cisplatin is one of the most potent antitumour drugs available for the therapeutic management of solid tumours, overian, lung, head, neck, and bladder cancers, etc. Despite wide application as a chemotherapeutic agent, cisplatin exhibits severe side effects, such as nephrotoxicity, neurotoxicity, ototoxicity, nausea, and emetogenicity, *etc.*, which limit possibilities for gaining therapeutic benefits from dose intensification [5,6]. Thus, scientists are now engaged to explore the transition metal based complexes and other metal based complexes. Hence, the higher degree of conjugated versatile ligand systems of the Knoevenagel condensate β-diketimine as Schiff bases containing electron releasing/electron withdrawing groups and their low molecular weight copper(II) and zinc(II) complexes have been synthesized. Study of their structure, spectral and redox properties as models for metalloproteins are essential in order to further address the structure–redox relationship. It is therefore of interest to carryout investigations on model compounds to understand how a ligand environment could affect the redox properties of the central metal and also interested to explore the DNA binding and DNA cleavage activity of synthesized complexes.

ISSN(Online) : 2319 - 8753
ISSN (Print) : 2347 - 6710

International Journal of Innovative Research in Science, Engineering and Technology

(An ISO 3297: 2007 Certified Organization)

Vol. 4, Issue 2, February 2015

II. MATERIALS AND METHODS

Materials and Instruments

All reagents and chemicals were procured from Merck products. DNA was purchased from Bangalore Genei (India). Agarose (molecular biology grade), ethidium bromide (EB) were obtained from Sigma (USA). Tris(hydroxymethyl)aminomethane–HCl (Tris–HCl) buffer solution was prepared using deionized, sonicated triply distilled water.

Carbon, hydrogen and nitrogen analysis of the complexes were carried out on a CHN analyzer CalrloErba 1108, Heraeus. The infrared spectra (KBr disks) of the samples were recorded on a Perkin–Elmer 783 series FTIR spectrophotometer. The electronic absorption spectra in the 200–1100 nm were obtained on a Shimadzu UV-1601 spectrophotometer. ^{1}H and ^{13}C NMR spectra (300 MHz) of the ligand and its zinc complexes were recorded on a BrukerAvance DRX 300 FTNMR spectrometer using $CDCl_3$ as solvent. Tetramethylsilane was used as internal standard. Fast atomic bombardment mass spectra (FAB-MS) were obtained using a VGZAB-HS spectrometer in a 3-nitrobenzylalcohol matrix. The X-band EPR spectra of the complexes were recorded at RT (300 K) and LNT (77 K) using DPPH as the g-marker. Molar conductance of 10^{-3} M solutions of the complexes in N,N'-dimethylformamide (DMF) were measured at room temperature with an Deepvision Model-601 digital direct reading deluxe conductivity meter. Magnetic susceptibility measurements were carried out by employing the Gouy method at room temperature on powder sample of the complex. $CuSO_4.5H_2O$ was used as calibrant. Electrochemical measurements were performed on a CHI 620C electrochemical analyzer with three electrode system of a glassy carbon electrode as the working electrode, a platinum wire as auxiliary electrode and Ag/AgCl as the reference electrode. Solutions were deoxygenated by purging with N_2 prior to measurements.

Synthesis of Ligands and Metal complexes

Synthesis of 3-(3-phenyl-allylidene)-pentane-2,4-dione

Pentane-2,4-dione (10 mmol) was mixed with 3-phenyl-propenal (10 mmol) and piperidine (0.2 mL), and the reaction mixture was stirred thoroughly for *ca*. 5 h with occasional cooling. Yellow colored crystalline solid was obtained after two weeks on keeping in the refrigerator which was filtered, washed with ethanol followed by an excess of petroleum-ether to remove any unreacted reagents. Washing was repeated for two or three times and then the compound was recrystallized from ethylacetate–petroleum ether mixture to get a pure yellow solid, Knoevenagel condensate [3-(3-phenyl-allylidene)-pentane-2,4-dione]. It was used as the starting material for the preparation of Schiff base.

Yield: 65%. IR (KBr pellet, cm^{-1}): 1718 ν(–C=O), 1570 ν(–HC=C). ^{1}H–NMR (δ): (aromatic, 7H) 6.9–7.3 (m); (–C=CH–, 1H), 8.2 (d); ($–CH_3$), 2.3 (s). ^{13}C–NMR (δ): 126.0–128.0 (C_1 to C_3), 138.4 (C_4), 129.0 (C_5), 125.7 (C_6), 146.9 (C_7), 145.2 (C_8), 197.5 (C_9), 24.5 (C_{10}). MS m/z (%): 215 $[M+1]^+$. Anal. Calc. for $C_{14}H_{14}O_2$: C, 78.5; H, 6.7; Found: C, 78.1; H, 6.2 (%). λ_{max} (cm^{-1}) in EtOH, 37986.

Synthesis of Schiff bases

The Schiff base was prepared by dissolving 3-(3-phenyl-allylidene)-pentane-2,4-dione (10 mmol) in ethanol and refluxed with *p*-substituted (X) aniline where X = $–NO_2$ (L^1), –H (L^2), –OH (L^3) and $–OCH_3$ (L^4) (20 mmol) in ethanol after the addition 0.5 g of anhydrous K_2CO_3 for *ca*. 6 h. The K_2CO_3 was filtered off from the reaction mixture. The dark brown solution was set aside to evaporate and the dark brown solid that separated was filtered off and recrystallized from ethanol and dried in *vacuo*.

L^1. Yield: 54%. IR (KBr pellet, cm^{-1}): 1629 ν(–C=N); 1580 ν(–HC=C); 1480, 1324, 864 ν(–C–N ring str; $–NO_2$). ^{1}H–NMR (δ): (aromatic) 6.8–7.2 (m); ($–CH_3$, 6H), 2.1 (s). ^{13}C–NMR (δ): 125.0–127.6 (C_1 to C_5), 137 (C_6), 116 (C_7), 161.4 (C_8), 18.9 (C_9), 152.5 (C_{10}), 121.9 (C_{11}), 123.6 (C_{12}), 146.8 (C_{13}). MS m/z (%): 455 $[M+1]^+$. Anal. Calc. for $C_{26}H_{22}N_4O_4$: C, 68.7; H, 4.9; N, 12.3; Found: C, 68.2; H, 4.9; N, 12.0 (%). λ_{max} (cm^{-1}) in EtOH, 46256, 27635.

L^2. Yield: 52%. IR (KBr pellet, cm^{-1}): 1586 ν(–HC=C–); 1632 ν(–C=N). ^{1}H–NMR (δ, ppm): (aromatic) 6.9–7.3 (m); ($–CH_3$, 6H), 2.5 (s). ^{13}C–NMR (δ, ppm):125.6–128.2 (C_1 to C_5 and C_{13}), 137 (C_6), 116 (C_7), 158.6 (C_8), 17.6 (C_9), 148.5 (C_{10}), 120.9 (C_{11}), 129.9 (C_{12}). MS m/z (%): 365 $[M+1]^+$. Anal. Calc. for $C_{26}H_{24}N_2$: C, 85.7; H, 6.6; N, 7.7; Found: C, 85.2; H, 6.6; N, 7.3 (%). λ_{max} (cm^{-1}) in EtOH, 41854, 28965.

L^3. Yield: 54%. IR (KBr pellet, cm^{-1}): 3434 ν(–OH); 1638 ν(–C=N); 1572 ν(–HC=C). ^{1}H–NMR (δ, ppm): (aromatic) 6.9-7.5 (m); (–OH, 1H) 10.8 (s); ($–CH_3$, 6H), 2.3 (s). ^{13}C–NMR (δ, ppm): 125.2–129.5 (C_1 to C_5), 137 (C_6), 116 (C_7),

ISSN(Online) : 2319 - 8753
ISSN (Print) : 2347 - 6710

International Journal of Innovative Research in Science, Engineering and Technology

(An ISO 3297: 2007 Certified Organization)

Vol. 4, Issue 2, February 2015

159.6 (C_8), 14.7 (C_9), 139.2 (C_{10}), 123.8 (C_{11}), 120.4 (C_{12}), 152.6 (C_{13}). MS m/z (%): 397 $[M+1]^+$. Anal. Calc. for $C_{26}H_{24}N_2O_2$: C, 78.6; H, 6.1; N, 7.1; Found: C, 78.1; H, 6.1; N, 7.0 (%). λ_{max} (cm^{-1}) in EtOH, 45298, 28269.
L^4. Yield: 47%. IR (KBr pellet, cm^{-1}): 1641 ν(–C=N); 1589 ν(–HC=C); 1284, 1086 ν(–C–O–C–). ^{1}H–NMR (δ): (aromatic) 6.9–7.3 (m); (–CH_3, 6H), 2.4 (s); 3.7 (–OCH_3, 6H). ^{13}C–NMR (δ):125.0–128.0 (C_1 to C_5), 137 (C_6), 116 (C_7), 159.4 (C_8), 16.9 (C_9), 141.8 (C_{10}), 123.3 (C_{11}), 116.2 (C_{12}), 154.6 (C_{13}), 59.5 (C_{14}). MS m/z (%): 425 $[M+1]^+$. Anal. Calc. for $C_{28}H_{28}N_2O_2$: C, 79.2; H, 6.7; N, 6.6; Found: C, 79.0; H, 6.7; N, 6.3 (%). λ_{max} (cm^{-1}) in EtOH, 42354, 28518.

Synthesis of metal complexes

To a stirred ethanolic solution of the above Schiff base(s) (5 mmol), a solution of copper(II)/zinc(II) chloride (5 mmol) in ethanol was added dropwise. The reaction solution was refluxed for 2 h. After cooling the reaction mixture to an ambient temperature, the formed solid was filtered, washed with diethyl ether and finally dried *in vacuum*.
$[CuL^1Cl_2]$. Yield: 42%. IR (KBr pellet, cm^{-1}): 1601 ν(–C=N); 1576 ν(–HC=C); 1475, 1326, 865 ν(–C–N str; –NO_2); 421 (M–N). MS m/z (%): 589 $[M]^+$. Anal. Calc. for $C_{26}H_{22}N_4O_4CuCl_2$: Cu, 10.9; C, 53.0; H, 3.8; N, 9.5; Found: Cu, 10.6; C, 52.7; H, 3.7; N, 9.3 (%). Λ_M 10^{-3} (ohm^{-1} cm^2 mol^{-1}) = 5.6. λ_{max} in DMF, 44345, 35428, 17815. μ_{eff} (BM): 1.81.
$[CuL^2Cl_2]$. Yield: 51%. IR (KBr pellet, cm^{-1}): 1612 ν(C=N); 1585 ν(–HC=C); 445 (M–N). MS m/z (%): 499 $[M]^+$. Anal. Calc. for $C_{26}H_{24}N_2CuCl_2$: Cu, 12.7; C, 62.6; H, 4.8; N, 5.6; Found: Cu, 12.4; C, 62.2; H, 4.8; N, 5.6 (%). Λ_M 10^{-3} (ohm^{-1} cm^2 mol^{-1}) = 9.0 λ_{max} (cm^{-1}) in DMF, 40816, 29876, 18956. μ_{eff} (BM): 1.86.
$[CuL^3Cl_2]$. Yield: 38%. IR (KBr pellet, cm^{-1}): 1611 ν(–C=N); 1570 ν(–HC=C); 3428 ν(–OH); 440 (M–N). MS m/z (%): 532 $[M+1]^+$. Anal. Calc. for $C_{26}H_{24}N_2O_2CuCl_2$: Cu, 12.0; C, 58.8; H, 4.6; N, 5.3; Found: Cu, 11.8; C, 58.6; H, 4.5; N, 5.3 (%). Λ_M 10^{-3} (ohm^{-1} cm^2 mol^{-1}) = 4.2. λ_{max} (cm^{-1}) in DMF, 41216, 31785, 17478. μ_{eff} (BM): 1.84.
$[CuL^4Cl_2]$. Yield: 49%. IR (KBr pellet, cm^{-1}): 1610 ν(–C=N); 1582 ν(–HC=C); 1276, 1083, ν(–C–O–C–); 419 (M–N). MS m/z (%): 559 $[M]^+$. Anal. Calc. for $C_{28}H_{28}N_2O_2CuCl_2$: Cu, 11.4; C, 60.2; H, 5.1; N, 5.0; Found: Cu, 11.2; C, 60.0; H, 5.0; N, 4.7 (%). Λ_M 10^{-3} (ohm^{-1} cm^2 mol^{-1}) = 3.7. λ_{max} (cm^{-1}) in DMF, 41256, 30129, 18489. μ_{eff} (BM): 1.83.
$[ZnL^1Cl_2]$. Yield: 47%. IR (KBr pellet, cm^{-1}): 1612 ν(–C=N); 1575 ν(–HC=C); 1473, 1324, 861 ν(–C–N str; –NO_2); 429 (M–N). ^{1}H–NMR (δ): (aromatic) 6.9–7.2 (m); (–CH_3, 6H). MS m/z (%): 591 $[M]^+$. Anal. Calc. for $C_{26}H_{22}N_4O_4ZnCl_2$: Zn, 11.1; C, 52.9; H, 3.8; N, 9.5; Found: Zn, 10.9; C, 52.6; H, 3.6; N, 9.2 (%). Λ_M 10^{-3} (ohm^{-1} cm^2 mol^{-1}) = 3.9. λ_{max} (cm^{-1}) in DMF, 42365, 32659. μ_{eff} (BM): diamagnetic.
$[ZnL^2Cl_2]$. Yield: 42%. IR (KBr pellet, cm^{-1}): 1606 ν(–C=N); 1581 ν(–HC=C); 451 (M–N). ^{1}H-NMR (δ): (aromatic) 6.8–7.1 (m); (–CH_3, 6H), 2.6 (s). MS m/z (%): 501 $[M]^+$. Anal. Calc. for $C_{26}H_{24}N_2ZnCl_2$: Zn, 13.1; C, 62.4; H, 4.8; N, 5.6; Found: Zn, 12.8; C, 62.1; H, 4.8; N, 5.2 (%). Λ_M 10^{-3} (ohm^{-1} cm^2 mol^{-1}) = 5.7. λ_{max} (cm^{-1}) in DMF, 40924, 29898. μ_{eff} (BM): diamagnetic.
$[ZnL^3Cl_2]$. Yield: 43%. IR (KBr pellet, cm^{-1}): 1616 ν(–C=N); 1571 ν(–HC=C); 3427 ν(–OH); 435 (M–N). ^{1}H–NMR (δ): (aromatic) 6.8–7.1 (m); ν(–OH, 1H), 10.7; (–CH_3, 6H), 2.3 (s). MS m/z (%): 533 $[M]^+$. Anal. Calc. for $C_{26}H_{24}N_2O_2ZnCl_2$: Zn, 12.3; C, 58.6; H, 4.5; N, 5.3; Found: Zn, 12.0; C, 58.4; H, 4.4; N, 5.0 (%). Λ_M 10^{-3} (ohm^{-1} cm^2 mol^{-1}) = 4.7. λ_{max} (cm^{-1}) in DMF, 41984, 33287. μ_{eff} (BM): diamagnetic.
$[ZnL^4Cl_2]$. Yield: 53%. IR (KBr pellet, cm^{-1}): 1616 ν(–C=N); 1581 ν(–HC=C); 1274, 1081 ν(–C–O–C–); 436 (M–N). ^{1}H-NMR (δ): (aromatic) 7.0–7.4 (m); (–OCH_3, 6H), 3.6(s); (–CH_3, 6H), 2.3 (s). MS m/z (%): 561 $[M]^+$. Anal. Calc. for $C_{28}H_{28}N_2O_2CuCl_2$: Zn, 11.7; C, 60.0; H, 5.0; N, 5.0; Found: Zn, 11.5; C, 59.7; H, 5.0; N, 4.7 (%). Λ_M 10^{-3} (ohm^{-1} cm^2 mol^{-1}) = 8.3. λ_{max} (cm^{-1}) in DMF, 42548, 31457. μ_{eff} (BM): diamagnetic.

III. EXPERIMENTAL RESULTS AND DISCUSSION

Infrared spectra

The IR spectra of the complexes were compared with the IR spectra of the ligand in order to ascertain the changes that might have taken place. The spectra of free ligands show a band in the region 1630-1610 cm^{-1} characteristics of the ν(C=N) stretching mode [7] indicating the formation of the Schiff base products. This band is shifted towards lower frequency by *ca.*20 cm^{-1} on complexation compared to free ligands indicating the involvement of the azomethine nitrogen in chelation with the metal ion, the coordination of the nitrogen to the metal ion would be expected to reduce the electron density of the azomethine link and thus causes a shift in the ν(C=N) group [8]. Coupled with this, the absence of a band around 1641–1730 cm^{-1} [21], characteristic of ν(–C=O) in 3-(3-phenyl-allylidene)-pentane-2,4-dione, suggests that the condensation of the keto groups is complete. The free –OH group of the ligand L^3 vibrated at *ca.* 3435

ISSN(Online) : 2319 - 8753
ISSN (Print) : 2347 - 6710

International Journal of Innovative Research in Science, Engineering and Technology

(An ISO 3297: 2007 Certified Organization)

Vol. 4, Issue 2, February 2015

cm^{-1} [9] does not show any significant shift on complex formation. Conclusive evidence of the bonding is also shown by the observation that new bands appear in the spectra of all metal complexes in the low frequency regions at 410–439 and 370–396 cm^{-1} characteristic for M–N and M–Cl vibrations, respectively, which are not observed in the spectra of free ligands.

Electronic absorption spectra

The electronic absorption spectra of the ligands and their complexes were recorded at 300 K in ethanol and DMF solution respectively.The free ligands exhibit two intense bands in 46256–41854 and 28965-27635 cm^{-1} region due to $\pi \rightarrow \pi^*$ and $n \rightarrow \pi^*$ transitions [10], respectively. In all the metal complexes, the absorption bands at 44345-40816 and 29876-35428 cm^{-1} are due to $\pi \rightarrow \pi^*$ and $n \rightarrow \pi^*$ transitions that are observed in the spectra of the free ligands L^1, L^2, L^3 and L^4. These transitions are shifted to blue or red frequencies due to the coordination of the ligand with metal ions. The electronic spectra of Cu(II) complexes show two broad, low intensity shoulder bands in the visible region, around 16152–19213 cm^{-1}, which are assigned to the combination of $^2B_{1g} \rightarrow {}^2A_{1g}$ and $^2B_{1g} \rightarrow {}^2E_g$ transitions respectively. The electronic spectral data suggest a square-planar geometry around the Cu(II) ion. The observed magnetic moment of the Cu(II) complexes (1.81-1.86 B.M) at room temperature indicates the non-coupled mononuclear complexes of magnetically diluted d^9 system with S=1/2 spin-state. The monomeric nature of the complexes is further supported by the microanalytical and ESI mass spectral data. The electronic absorption spectra of the diamagnetic Zn(II) complexes show the bands at 40924–42548 and 29898–33287 cm^{-1} which are assigned to intra-ligand charge transfer transitions [11].

NMR spectra of zinc complexes

The ^1H NMR spectra of ligands and their diamagnetic Zn(II) complexes were recorded in$CDCl_3$. In ^1H NMR, the aromatic region is a set of mutiplets in the range of 6.8-7.8 ppm for all the ligands and their Zn(II) complexes. The phenolic –OH proton for L^3 ligand and its zinc complexes was observed as a singlet at *ca.* 10.8 and 10.7 ppm respectively. It is suggesting that phenolic –OH group is not taking part in the complexation. ^1H NMR spectra of aliphatic methyl protons exhibit at 2.1-2.6 ppm for all the Schiff base ligands and their Zn(II) complexes.

The decoupled ^{13}C NMR (in $CDCl_3$ for ligands and their complexes) confirm the presence of imine functions and in all cases the spectra are in accordance with assigned structure. Comparison of all carbon peaks of the ligands with those of zinc complexes shows some upfield and downfield shifts, but these shifts are not large. This indicates the coordination of the ligand to the metal ion.

Mass spectra

The mass spectrum of L^1 ligand shows M+1 peak at m/z 455 (54.6 %) corresponding to $[C_{26}H_{24}N_2O_2]^+$ ion.Also, the spectrum exhibits the fragments at m/z 107, 77 and 66 corresponding to $[C_6H_5NO]^+$, $[C_6H_5]^+$ and $[C_5H_6]^+$ respectively. The mass spectrum of $[ZnL^1Cl_2]$shows peaks at m/z 597 and 598 with 39.8 and 35.7 % abundances, respectively. The peak at m/z 597 may represent the molecular ion peak of the complex and the other peaks are isotopic species. The strongest peaks (base beak) at m/z455 represent the stable species $C_{26}H_{24}N_2O_2$. The m/z of all the fragments of ligandsand their complexes confirm the stoichiometry of the complexes as $[MLCl_2]$. The observed peaks are in good agreement with their formulae as expressed from microanalytical data. Thus, the mass spectral data reinforce the conclusion drawn from the analytical and conductance values.

EPR spectral study

The X-band EPR spectra of all copper(II) complexes have been recorded in DMSO at liquid nitrogen temperature and at room temperature. The EPR spectra of the copper(II) complexes at room temperature show one intense absorption band in the high field and is isotropic due to the tumbling motion of the molecules. However, these complexes at liquid nitrogen temperature show four well-resolved peaks with low intensities in the low field region and one intense peak in the high field region. From this spectral data, it is found that $A_{\parallel}$ (135-150) $>A_{\perp}$(46-52); $g_{\parallel}$ (2.12-2.26) $>g_{\perp}$(2.01-2.06)> 2.0027, which support the $d_{x^2-y^2}$ as the ground state, characteristic of square-planar geometry and axially symmetric.The *G* values lie within the range 4.6–5.2 for all the copper complexes indicating negligible exchange interaction of Cu–Cu in the complexes according to Hathaway [12].The degree of geometrical distortion is ascertained by the parameter $g_{\parallel}/A_{\parallel}$ ($A_{\parallel}$ in cm^{-1}) with the values less than140 cm^{-1} associated with the square-planar structures, whereas higher values indicate distortion towards tetrahedron [13]. For the present copper complexes, the $g_{\parallel}/A_{\parallel}$ values found in the range of

ISSN(Online) : 2319 - 8753
ISSN (Print) : 2347 - 6710

International Journal of Innovative Research in Science, Engineering and Technology

(An ISO 3297: 2007 Certified Organization)

Vol. 4, Issue 2, February 2015

154–174 cm^{-1} are in agreement with significant deviation from planarity which is further confirmed by the bonding parameter α^2 whose value is less than unity.The EPR study of the copper(II) complexes has provided supportive evidence to the conclusion obtained on the basis of electronic and magnetic moment values.
Based on the above analytical and spectral data, the structure of the ligands and their complexes is shown in Fig. 1 and Fig. 2 respectively.

where X = $-NO_2$ (L^1), -H (L^2), -

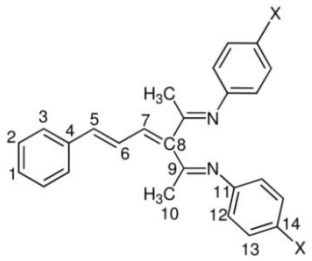

OH (L^3) and $-OCH_3$ (L^4)

Fig. 1. Structure of ligands

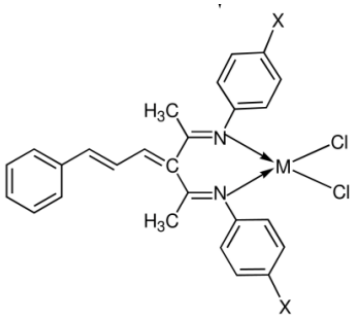

where X = $-NO_2$ (L^1), -H (L^2), -OH (L^3) and $-OCH_3$ (L^4), M = Cu(II)/Zn(II)

Fig. 2. Structure of complexes

DNA binding studies

Electronic spectral studies

Electronic absorption spectroscopy is widely employed to determine the DNA binding affinity of metal complexes. The present copper(II) complexes do not exhibit any intense d–d or charge transfer band to monitor their interaction with DNA. So the intense ligand based π–π* absorption band is used to monitor the interaction of the complexes with calf thymus DNA. Complexes bound to DNA through intercalation, which involves a strong stacking interaction of the planar aromatic rings of the coordinated ligand with the base pairs of DNA, usually result in hypochromism and red shift of ligand-band or charge transfer bands [13]. All the present complexes exhibit significant hypochromism(15–27%) on the incremental addition of DNA with varying red shifts (Fig. 3, Table 1). Further, as the extent of hypochromism is commonly consistent with the strength of intercalative interaction, it is evident that all the complexes exhibit almost the same DNA binding affinities [14]. All these observations reveal that the present complexes intercalate less strongly. Moreover, the uncoordinated substituted group of the ligand chain may be involved in secondary interactions like hydrogen bonding with DNA possessing several hydrogen bonding sites accessible both in the minor and major grooves [15]. Similar hydrogen bonding interactions have been proposed for $[Co(NH_3)_6]^{3+}$ bound to $d(CG)_3$ [16].

ISSN(Online) : 2319 - 8753
ISSN (Print) : 2347 - 6710

International Journal of Innovative Research in Science, Engineering and Technology

(An ISO 3297: 2007 Certified Organization)

Vol. 4, Issue 2, February 2015

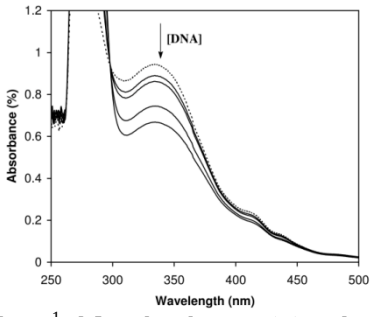

Fig. 3. Electronic absorption spectrum of $[CuL^1Cl_2]$ in the absence (--) and presence (–) of increasing amounts of DNA

Table 1 Absorption spectral properties of synthesized complexes

SI. No	Complexes	λ_{max} (nm)		$\Delta\lambda$ (nm)	%H	$K_b \times 10^3$ (M^{-1})
		Free	Bound			
1	$[CuL^1Cl_2]$	328.0	330.6	2.6	10	1.1
2	$[CuL^2Cl_2]$	320.0	321.0	1.0	6	0.4
3	$[CuL^3Cl_2]$	325.5	326.8	1.3	8	0.6
4	$[CuL^4Cl_2]$	322.6	323.8	1.2	9	0.5
5	$[ZnL^1Cl_2]$	329.5	331.5	2.0	9	1.0
6	$[ZnL^2Cl_2]$	321.4	322.4	1.0	7	0.2
7	$[ZnL^3Cl_2]$	326.3	327.1	0.8	8	0.7
8	$[ZnL^4Cl_2]$	323.7	324.6	0.9	6	0.6

In order to compare the binding strength of the complexes with CT DNA, the intrinsic binding constants K_b are obtained by monitoring the changes in absorbance for the complexes with increasing concentration of DNA. The K_b values of complexes are shown in Table 1. The binding strength of the synthesized complexes with DNA is shown as in the following order: $–NO_2$> –H > –OH > $–OCH_3$.

Electrochemical behaviour

The cyclic voltammograms of all the copper complexes were recorded in DMF with CHI620C at room temperature. The electrochemical data are given in Table 2. All these complexes show one well-defined redox couple corresponding to copper(II)/copper(I), as expected [17]. The measured ΔEp values (85–340 mV) clearly indicate that these redox couples are quasireversible. The I_{pa}/I_{pc} falls at ca. 0.9–1.1, clearly confirming one electron transfer in this redox process. The cyclic voltammogram of copper complexes in the absence and presence DNA is shown in Fig. 4. The complexes have been found to show an almost reversible electrochemical wave in the buffer with $E_{1/2}$ of 0.515–0.295 V *versus* Ag/AgCl. Presence of DNA causes a considerable decrease in the voltammetric current of the redox wave with a slight shift in $E_{1/2}$ to less negative potential. The drop of the voltammetric currents in the presence of DNA may be attributed to slow diffusion of the metal complex bound to CT DNA. This in turn indicates the extent of binding affinity of the complex to DNA. The net shift in $E_{1/2}$ can be used to estimate the ratio of equilibrium constants for the binding of the 2+ and 1+ ions to DNA. The Nernst equation for the reversible redox reactions of the free and bound species and the corresponding equilibrium constants for binding of each oxidation state to DNA for one electron redox process is given as follows:

$$CuL^{2+} + e^- \rightleftharpoons CuL^{+} \quad E^{o,}_f$$

$$K_{2+} \quad\quad K_{+}$$

$$CuL^{2+}\text{-DNA} + e^- \rightleftharpoons CuL^{+}\text{-DNA} \quad E^{o,}_b$$

Thus for the one electron process,

$E_b^{o'} - E_f^{o'} = 0.059 \log(K_+/K_{2+})$

ISSN(Online) : 2319 - 8753
ISSN (Print) : 2347 - 6710

International Journal of Innovative Research in Science, Engineering and Technology

(An ISO 3297: 2007 Certified Organization)

Vol. 4, Issue 2, February 2015

The ratio of equilibrium constants for the binding of the 1+ and 2+ ions to DNA was estimated to be less than unity. The value of K_{+}/K_{2+} indicates that the complex in its +2 oxidation state has slightly higher affinity to DNA compared to the complex in its +1 oxidation state. These results demonstrate that rather straight forward electrochemical methods can be employed to characterize the intercalative interaction between metal complexes or electro active species and DNA.

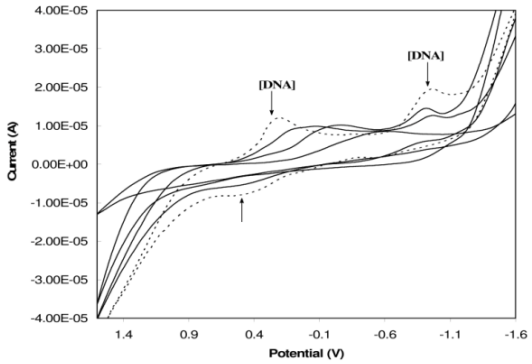

Fig. 4. Redox behaviour of $[CuL^{1}Cl_2]$ in the absence (---) and presence (—) of increasing amounts of DNA

Table 2 Electrochemical parameters of interaction of DNA with copper complexes

SI. No	Complexes	ΔEp (V)		$E_{1/2}$ (V)		Decrease of I_{pc} (%)	I_{pa}/I_{pc}		K_{+}/K_{2+}
		Free	Bound	Free	Bound		Free	Bound	
1	$[CuL^{1}Cl_2]$	0.139	0.130	0.515	0.498	18	0.92	0.85	0.84
2	$[CuL^{2}Cl_2]$	0.189	0.181	0.343	0.331	13	0.96	0.87	0.89
3	$[CuL^{3}Cl_2]$	0.324	0.315	0.349	0.338	10	0.93	0.89	0.97
4	$[CuL^{4}Cl_2]$	0.337	0.324	0.307	0.295	11	0.91	0.88	0.91

The electrochemical behaviour of all the zinc complexes in the absence of DNA shows only cathodic potential corresponding to Zn(II)/Zn(0). The cathodic peak appears negative potential of 0.606 to 0.748 V range corresponds to the two electron reduction of Zn(II) complexes. Addition of CT DNA to the solution of zinc complexes results in a shift of cathodic peak potentials to more negative values and a decrease of the cathodic currents. The shift of the cathodic potential of the complexes in the presence of DNA to more negative values indicates a binding interaction between the complexes and DNA that makes the complexes less readily reducible. The drop of the voltammetric currents in the presence of CT DNA can be attributed to diffusion of metal complexes bound to higher and slowly diffusing DNA molecule. The decreased extents of the peak currents (Table 3) observed for the complexes upon addition of DNA may indicate copper complexes possess more DNA-binding affinity than zinc complexes. Peak potentials of zinc complexes were independent of sweep rate (50–500 mV/s) and ΔEp values were between 63 and 76 mV.

Differential pulse voltammogram of the Zn(II) complexes observed a negative potential shift along with significant decreasing of current intensity during the addition of increasing amounts of DNA. It indicates that zinc ions stabilize the duplex (GC pairs) by intercalating way.

The dissociation constant (K_d) of the Zn(II)-DNA complex was obtained using the following equation:

$$i_p^2 = \frac{K_d}{[DNA]}\left(i_{po}^2 - i_p^2\right) + i_{po}^2 - [DNA]$$

whereK_d is dissociation constant of the complex Zn(II)-DNA, i^2_po and i^2_p are reduction current of Zn(II) in the absence and presence of DNA respectively. The low dissociation constant values (Table 3) of Zn(II) ions are indispensable for structural stability of Zn(II)-DNA adduct which participates in the replication, degradation and translation of genetic material of all species.

ISSN(Online) : 2319 - 8753
ISSN (Print) : 2347 - 6710

International Journal of Innovative Research in Science, Engineering and Technology

(An ISO 3297: 2007 Certified Organization)

Vol. 4, Issue 2, February 2015

Table 3 Electrochemical parameters for the interaction of DNA with zinc complexes

SI.No	Complexes	Ep (V)		I_{pc} (μA)		$K_d \times 10^{-9}$ ($molL^{-1}$)
		Free	Bound	Free	Bound	
1	$[ZnL^1Cl_2]$	0.748	0.736	0.74	0.30	1.3
2	$[ZnL^2Cl_2]$	0.698	0.685	0.65	0.42	1.4
3	$[ZnL^3Cl_2]$	0.657	0.650	0.50	0.34	1.1
4	$[ZnL^4Cl_2]$	0.606	0.598	0.43	0.30	1.5

DNA cleavage

From Fig. 5a and Fig. 5b, it is evident that the hydroxyl radical scavenger, DMSO, significantly diminished the nuclease activity of copper complexes, which indicates the involvement of the diffusible hydroxyl radical in the cleavage process. Sodium azide, scavenger of singlet oxygen or singlet oxygen-like species, both reduce the DNA damage by introducing the participation of the singlet oxygen or a singlet oxygen-like entity. Tiron, a scavenger of superoxide anion, also inhibits DNA damage, thus proving that this reactive oxygen species is involved in the DNA cleavage.

Lane 1 2 3 4 5 6 7 8

Fig. 5a. Gel electrophoresis diagram showing the cleavage of SC pUC19 DNA (0.2 μg) by the synthesized complexes (50 μM) in the presence of MPA (5 mM): lane 1, DNA control; lane 2, DNA + L^1 (50 μM); lane 3, DNA + $[CuL^1Cl_2)]$ + MPA; lane 4, DNA + $[CuL^1Cl_2]$; lane 5, DNA + $[CuL^1Cl_2]$ + DMSO (4 μL) + MPA; lane 6, DNA + $[CuL^1Cl_2]$ + NaN_3 + MPA; lane 7, DNA + $[CuL^1Cl_2]$ + distamycin (50 μM) + MPA; lane 8, DNA + $[CuL^1Cl_2]$ + MPA + SOD (1 U)

Lane 1 2 3 4 5 6 7 8

Fig. 5b. Gel electrophoresis diagram showing the cleavage of SC pUC19 DNA (0.2 μg) by the synthesized complexes (50 μM) in the presence of MPA (5 mM): lane 1, DNA + $[CuL^2Cl_2]$ + H_2O_2; lane 2, DNA + L^2 (50 μM); lane 3, DNA + $[CuL^3Cl_2]$ + MPA; lane 4, DNA + $[CuL^3Cl_2]$ + DMSO (4 μL); lane 5, DNA + $[CuL^4Cl_2]$ + MPA; lane 6, DNA + L^4; lane 7, DNA + $[CuL^4Cl_2]$ + distamycin (50 μM) + MPA; lane 8, DNA + $[CuL^4Cl_2]$ + MPA + NaN_3

In fact, the SOD enzyme actually increases the nuclease process, which suggests that in this case the dismutation of the superoxide produced by the enzyme gives rise to ROS which breaks the DNA strands to a greater extent than the complexes plus reducing agents. The presence of distamycin, respective binder of the minor groove of DNA, does inhibit the breakage of DNA strands, thus implying that complexes interact with DNA in the minor groove.

Hydrogen peroxide can also react with another equivalent of Cu(I)L to produce hydroxyl radical-species which could be metal bound. This species, which may be considered analogous to a metal-oxo system, is responsible for initiating DNA strand scission chemistry [18].

IV. CONCLUSIONS

Novel copper(II) and zinc(II) complexes of the type $[MLCl_2]$, [L = Schiff base derived from the condensation of 3-(3-phenyl-allylidene)-pentane-2,4-dione and *p*-substituted (X) aniline; X = $–NO_2$ (L^1), –H (L^2), –OH (L^3) and $–OCH_3$ (L^4)] have been synthesized and structurally characterized. They have adopted square-planar geometry around the central metal ion. The planarities, flexible and extended conjugation of the ligands containing substituted groups have a profound effect on redox behaviour, DNA binding and cleavage of the complexes. Mechanistic investigations show a minor groove binding for the synthesized complexes with DNA. DNA cleavage activity of the synthesized copper complexes in the presence of a reducing agent, 3-mercaptopropionic acid and oxidizing agent, hydrogen peroxide *via* mechanistic pathway involves the formation of hydroxyl radical as the reactive species.

ISSN(Online) : 2319 - 8753
ISSN (Print) : 2347 - 6710

International Journal of Innovative Research in Science, Engineering and Technology

(An ISO 3297: 2007 Certified Organization)

Vol. 4, Issue 2, February 2015

V. ACKNOWLEDGEMENTS

The authors express their sincere thanks to the Head, Department of Chemistry, Principal and College Managing Board of Dr.Zakir Husain College, Ilayangudi and VHNSN College, Virudhunagar for their constant encouragement and providing research facilities.

REFERENCES

1. Tilala1, D., Gohel, H., Dhinoja, V.,Solanki, M., and Karia, D., "DNA Interaction and Antimicrobial Activities of New Complexes of Fe(II), Co(II), Ni(II) and Cu(II) That Incorporate Modifiede Acetyl &AcetoacetylBenzopyran Ligands", International Journal of Pharmacy & Technology, Vol. 5, No.2, pp. 5555 – 5566, 2013
2. Raman, N.,Jeyamurugan, R.,Sakthivel, A.,and Mitu, L., "Novel Metal-Based Pharmacologically Dynamic Agents of Transition Metal(II) Complexes: Designing, Synthesis, Structural Elucidation, DNA Binding and Photo-Induced DNA Cleavage Activity, Vol. 75, No. 1, pp. 88 – 97, 2010
3. SangeethaGowda, K.R., Mathew, B.B., Sudhamani, C.N., and BhojyaNaik, H.S., "Mechanism of DNA Binding and Cleavage", Biomedicine and Biotechnology, Vol.2, No. 1, pp. 1 -9, 2014.
4. Sun, Y.G., Yu, W., Wang, L., Rong, S.T., Wu, Y.L., Zhu, M.C., and Gao, E.J., "Synthesis and Crystal Structure of Complex $[Mn(Imdc)_2(H_2O)_2] \cdot 2H_2O$ and Its Interaction with DNA", Russian Journal of Coordination Chemistry, Vol. 36, No. 1, pp. 43-47, 2010
5. Galluzzi, L., Vitale, I.,Michels, J., Brenner, C., Szabadkai, G., Harel-Bellan, A., Catedo, M., and Kroemer, G., "Systems Biology of Cisplatin Resistance: Past, Present and Future",Cell Death Diseases, Vol. 5, No. 5, pp. 1257-1259, 2014.
6. Ali, I., Wani, W.A., Saleem, K., and Haque, A., "Platinum Compounds: A Hope for Future Cancer Chemotherapy", Anti-Cancer Agents in Medicinal Chemistry, Vol. 13, pp. 296 – 306, 2013.
7. Raman, N., Joseph, J., Sakthivel, A., and Jeyamurugan, R., "Synthesis, Structural Characterization and Antimicrobial Studies of Novel Schiff Base Copper(II) Complexes", Journal of Chilean Chemical Society, Vol. 54, No. 4, pp. 354 -357, 2009.
8. Abd El-Wahab, Z.H.,Mashaly, M.M., Salman, A.A., El-Shetary, B.A., and Faheim, A.A., "Co(II), Ce(III) and UO_2(VI) Bis-salicylatothiosemicarbazide Complexes: Binary and Ternary Complexes, Thermal Studies and Antimicrobial Activity", SpectrochimicaActa, A Molecular Biomolecular Spectroscopy, Vol.60, No. 12, pp. 2861- 2873, 2004.
9. Beinert,H., "Copper in Biological Systems", Journal of Inorganic Biochemistry, Vol. 44, No. 3,pp. 173-218, 1991
10. Lever, A.B.P.,"Inorganic Electronic Spectroscopy", Elsevier, Amesterdam, Vol. 33, 1984.
11. Addison, A.W.,Rao, T.N., and Sinn, E., "Spectroscopy and Structure of Thiolate and Thioether Complexes of Copper(II) and the Relationship of their Redox Properties of Certain Copper Proteins", Inorganic Chemistry, Vol. 23, pp.1957-1967, 1984.
12. Ray, R.K., and Kauffman, G.B., "EPR Spectra and Covalency of Bis-(amidinourea/O-alkyl-1-amidinourea)copper(II) Complexes. Part II. Properties of the CuN42- Chromophore," InorganicaChimicaActa, Vol. 173, No. 2, pp. 207–214, 1990.
13. Bloomfield, V.A., Crothers, D.M., and Tinocco, I.," Physical Chemistry of Nucleic Acids", Harper & Row Ed., New York, pp. 417 - 432, 1974.
14. Tysoe, S.A., Morgan, R.J., Baker, A.D., and Strekas, T.C., "Spectroscopic Investigation of Differential Binding Modes of Delta and Lambda-$Ru(bpy)_2ppz$ (2+) with Calf Thymus DNA", Journal of Physical Chemistry, Vol. 97, pp. 1707-1711, 1993.
15. Hong, X.L., Liang, Z.H., and Zeng, M.H., "Ruthenium(II) Complexes: Structure, DNA-binding, Photocleavage, Antioxidant Activity and Theoretical Studies", Journal of Coordination Chemistry, Vol. 64, Issue 21, pp. 3792-3807, 2011.
16. Gessner, R.V., Quigley, G.J., Wang, A.H.J., Van der Marel, G.A., Van Boom, J.H., and Rich, A., "Structural Basis for Stabilization of Z-DNA by Cobalt hexaammine and Magnesium Cations", Biochemistry, Vol. 24, No. 2, pp. 237–240, 1985.
17. Jeyasubramanian, K., Thambidurai, S.,Ramalingam, S.K., and Murugesan, R., "Spectral and Redox Models for Blue Copper Proteins: Copper(II) Complexes of β-diketonimines from a KnoevenagelCondensate", Journal of Inorganic Biochemistry, Vol. 72, No. 3, pp. 101-107, 1998.
18. Fenton, H.J.H.J., "Oxidation of Tartaric Acid in Presence of Iron", Journal of Chemical Society, Vol. 65, No. 65, pp. 899–911, 1894.